

Imaging Dose in Megavoltage (MV) and Kilovoltage (kV) Energy Ranges between 2D and 3D Image-Guided Radiation Therapy (IGRT): Phantom Study

Jayapramila Jayamani¹, Loo Yu Rou¹ and Reduan Abdullah²

¹*Medical Radiation Programme, School of Health Sciences, Health Campus, Universiti Sains Malaysia, 16150 Kubang Kerian, Kelantan, Malaysia*

²*Radiotherapy Department, Hospital Universiti Sains Malaysia, Health Campus, 16150 Kubang Kerian, Kelantan, Malaysia.*

Health Campus, Universiti Sains Malaysia





Medical Radiation Programme,
School of Health Sciences, Health Campus

COMMITTED TO HEALTH



Teaching Hospital



Background & Introduction

Based on worldwide cancer statistic done by IARC, breast cancer contributed the highest incidence cases (22.6 million cases) and followed by lung cancer (22.0 million cases).¹

IGRT ensures the accuracy of radiotherapy treatment by comparing patient's geometric on treatment day based on the planning CT images acquired during simulation.²

MOH: Image verification is performed within the first 3 fractions, followed by weekly except for SBRT, Cyberknife and tomotherapy as these techniques require more frequent verification.³

IGRT technique is divided into 2D and 3D imaging technique using different energy ranges.⁴

MV orthogonal

2D IGRT

kV orthogonal

kV Cone Beam Computed Tomography (kV CBCT)

3D IGRT

IGRT technique is chosen based on the treatment technique, target margin, image modality and available staff skills.⁵

IGRT techniques lead to different image quality and imaging dose accumulation at organ at risk (OAR) which eventually induce secondary cancer risk.⁶

This study will investigate the point dose and effective dose in the organs at the chest region such as lungs, heart, breast and skin contributed by 2D and 3D IGRT techniques using MV and kV energy ranges.

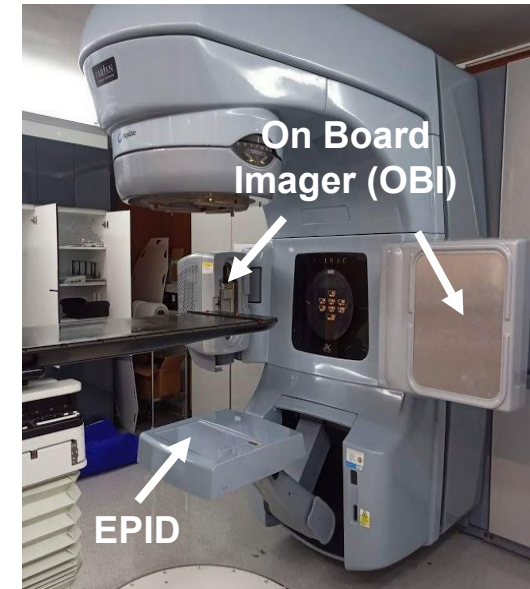


Figure 1: Varian Clinac iX linear accelerator (LINAC)

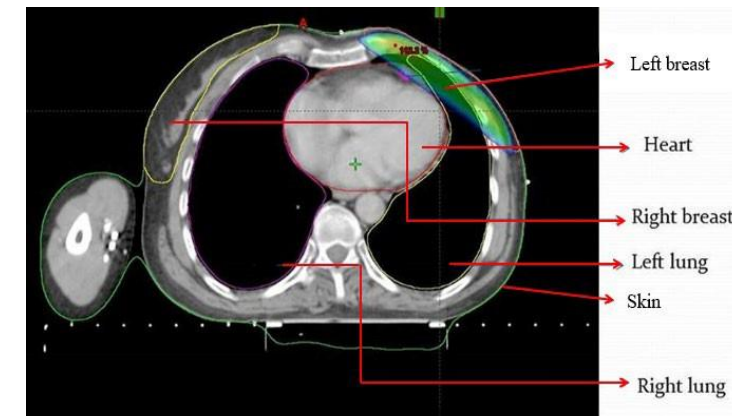


Figure 2: OAR at chest region

Problem Statement

Issue	Comment
Image Quality	<ul style="list-style-type: none"> • 3D IGRT generates superior image quality than 2D IGRT.⁷ • kV imaging produces better image quality than MV imaging.⁸
Accumulated Imaging Dose	<ul style="list-style-type: none"> • Imaging process is always associated with the imaging dose due to usage of ionizing radiation in MV and kV energy.⁶ • The imaging dose is accumulated in the OAR and eventually caused secondary malignancies.⁹ • The estimated excess absolute risk (EAR) for developing a secondary carcinoma at lung due to IGRT procedure is 1 to 10 cases per 10000 patient-year.⁹
Imaging Dose Reporting	<ul style="list-style-type: none"> • AAPM TG 75 suggested to compare the imaging dose between different techniques in term of effective dose but most of the studies reported in point dose only.⁴ • The imaging dose is ignored in the treatment planning as it is substantially lower than therapeutic dose.

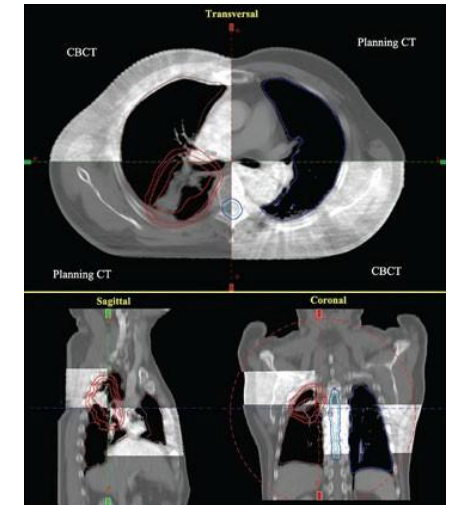


Figure 3: Chest region 3D images in axial (left), coronal (centre) & sagittal (right) acquired using 3D IGRT.⁷

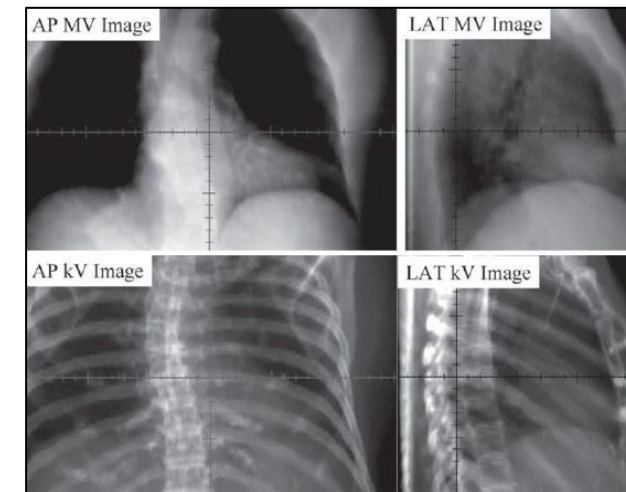


Figure 4: Chest region 2D images acquired in 2D IGRT using MV (top) and kV energy ranges (below).⁸

General Objective:

To investigate the imaging dose in MV and kV energy ranges between 2D and 3D IGRT techniques in the chest region.

Specific Objective:

- 1) To **evaluate** the image quality at chest region of an anthropomorphic phantom using MV and kV energy ranges in both 2D and 3D IGRT techniques
- 2) To **measure** the point dose received by the OAR in the chest region of the anthropomorphic phantom using thermoluminescent dosimeter (TLD-100H) under 2D and 3D IGRT techniques.
- 3) To **calculate** the effective dose of OAR at the chest region delivered by the MV and kV energy ranges in 2D and 3D IGRT techniques.

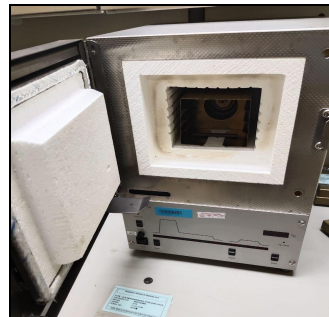
Calibration of TLD-100H



Varian Clinac iX LINAC with mounted EPID and OBI v1.6



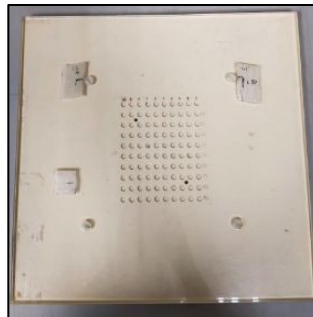
TLD-100H



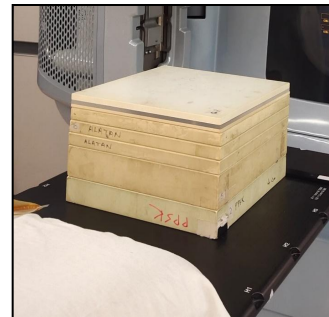
PTW T1231/U100 TLD Annealing Oven



Harshaw TLD Model 3500 Reader



TLD irradiation plate



Solid water phantom



PTW 30006/30013 Farmer cylindrical ionization chamber

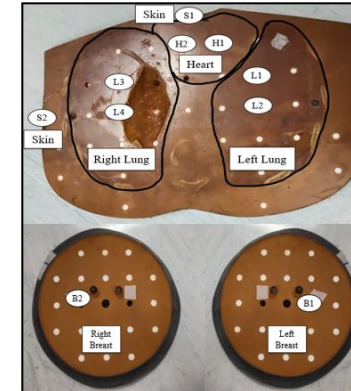


PTW-UNIDOS E electrometer

Point Dose Measurement



Anthropomorphic phantom- Chest region



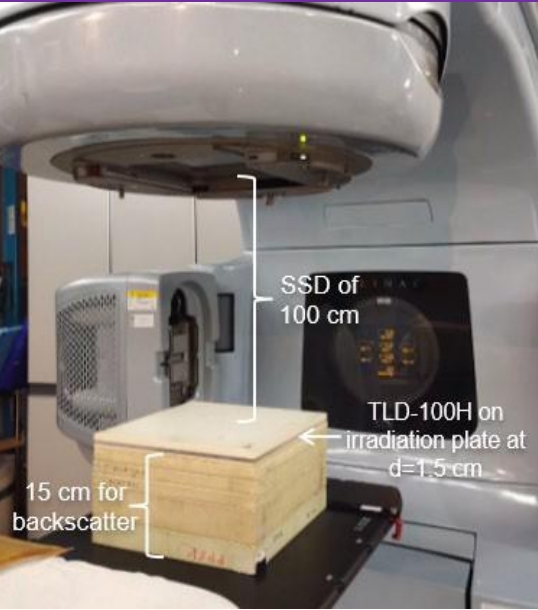
Philips Brilliance CT simulator

MV Energy ← Calibration of TLD-100H → kV Energy

Table 1: Parameter for MV energy calibration

SSD	100 cm
Field size	10 cm x 10 cm
Dmax	1.5 cm
Monitor unit	100 MU

Figure 6: MV energy calibration setup of TLD-100H.



1. 33 TLD-100H were calibrated under LINAC using 6 MV energy based on standard calibration setup (TRS398) (Figure 6).
2. The TLD-100H were annealed at 240 for 10 minutes and cooled down to room temperature for 1 hour.
3. The TLD-100H exposed to parameter stated in Table 1.
4. After 24 hours, TLD-100H were readout and annealed.
5. Step repeated 3 times.

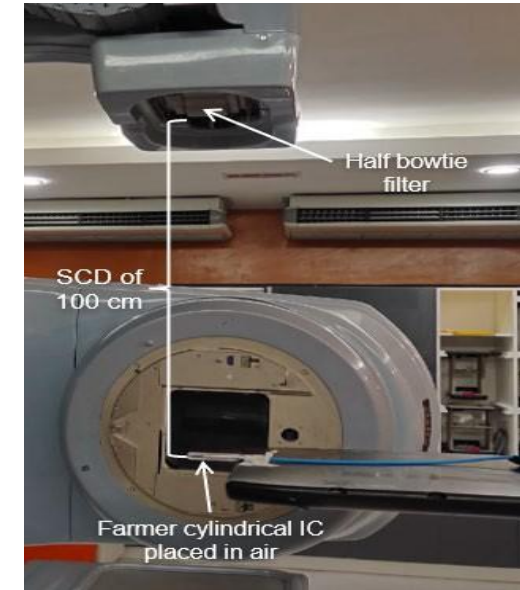
Dose Linearity

1. 33 TLD-100H were sorted based on sensitivity and divided into 11 groups, each group consists 3 TLD-100H.
2. The TLD-100H were exposed to different doses in the ranges between 0 mGy and 2000 mGy.

Table 2: Parameter for kV energy calibration

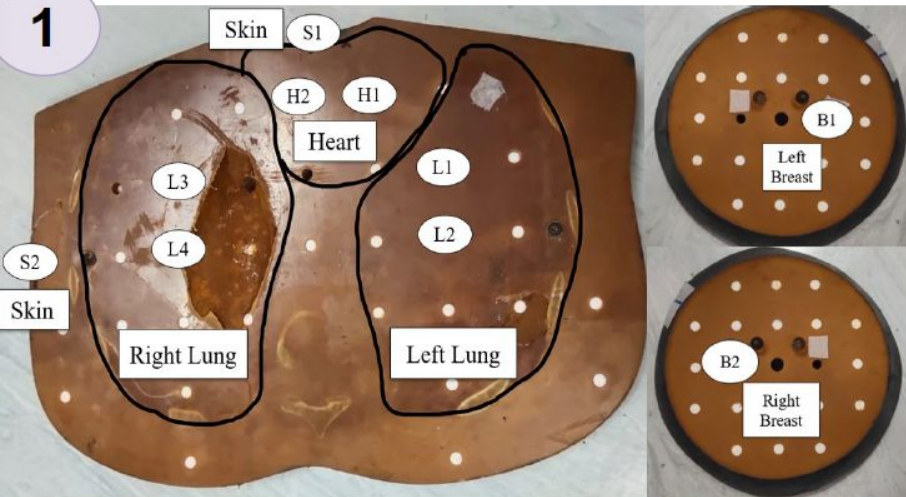
SCD	100 cm
Filter	Half bowtie
HVL	5.2 mm Al
Parameter	110 kV 20 mAs

Figure 7: kV energy calibration setup of TLD-100H.

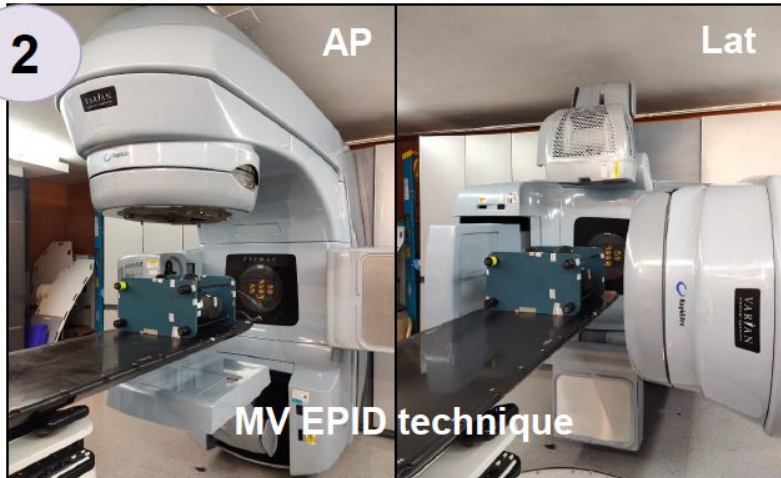


1. 33 TLD-100H were calibrated using Farmer IC using in-air method (Figure 7).
2. The Farmer IC was exposed to the parameter (Table 2) by changing various polarities and voltages for correction factors and absorbed dose to water in air, $D_{w,z=0cm}$ calculation.
3. The TLD-100H were sealed into plastic sachet and placed around the IC.
4. The TLD-100H was exposed to same parameter.
5. After 24 hours, TLD-100H were readout and annealed.

Part B: Point Dose Measurement



10 TLD-100H were placed at 10 point positions with label. A TLD-100H was used for background reading.



The TLD-100H was exposed to AP and Lat projections with 2 MU each projection.

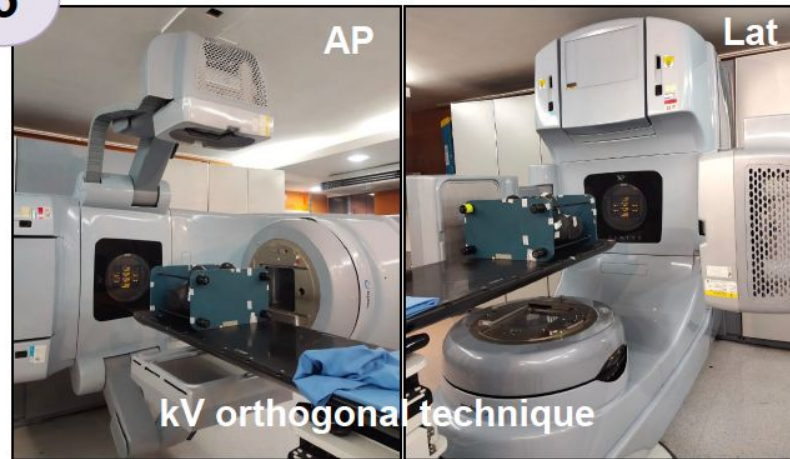
3

The measurement was repeated 3 times using another set of TLD-100H.

4

Step 1 – 3 was repeated for kV orthogonal and kV CBCT techniques with different exposure parameters.

5



The TLD-100H was exposed to AP (75 kV 5 mAs) and Lat projections (90 kV 40 mAs).

6



The TLD-100H was exposed to 110 kV, 262 mAs and half bowtie filter.

7

The image of anthropomorphic phantom at chest region was evaluated qualitatively.

8 Each TLD-100H charge was converted into dose using Eq 1.

$$\text{Dose} = \text{TLD reading} \times \text{ECC} \times \text{Individual Calibration factor} \quad \text{Eq 1}$$

ECC=Element correction coefficient

9 Since 3 TLD-100H was exposed at the same point position, the mean point dose ($D_{T,R}$) for each point position was averaged from 3 TLD-100H.

10 The mean point dose was converted into effective dose using Eq 2 for individual organ

$$E = \sum w_T \cdot \sum w_R \cdot D_{T,R} \quad \text{Eq 2}$$

w_T = Tissue weighting factor
 w_R = Radiation weighting factor (photon=1)
 $D_{T,R}$ = mean point dose

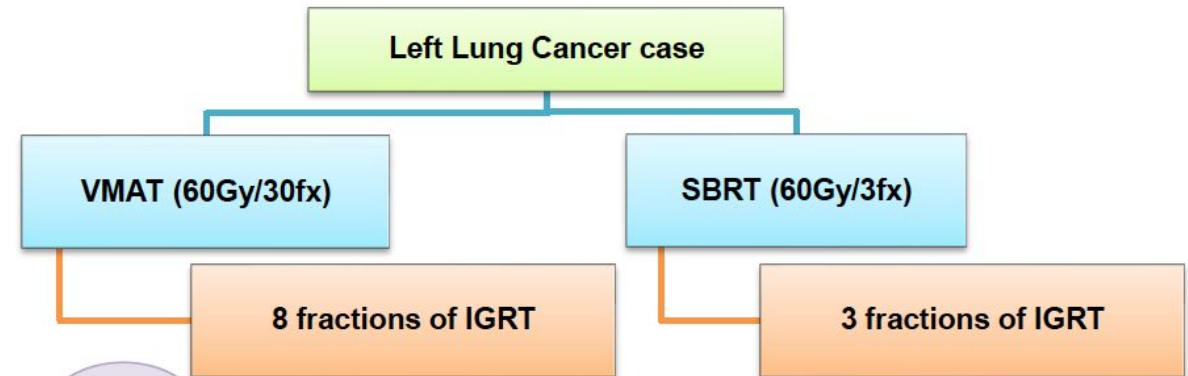
Organ	w_T
Lung	0.12
Heart	0.12
Breast	0.12
Skin	0.01

11 Analysis

- The mean point dose between 2D IGRT was analysed using independent sample t-test with significance level of 0.05
- The mean point dose between 2D and 3D IGRT technique was analysed using one-way ANOVA, the difference was considered significant when p values ≤ 0.05 .

12

- The effective dose between 2D and 3D IGRT was analysed using percentage error bar.



13

The point dose from single fraction of IGRT was multiplied to 8 and 3 fractions to obtain the accumulated dose.

Dose Linearity of TLD-100H

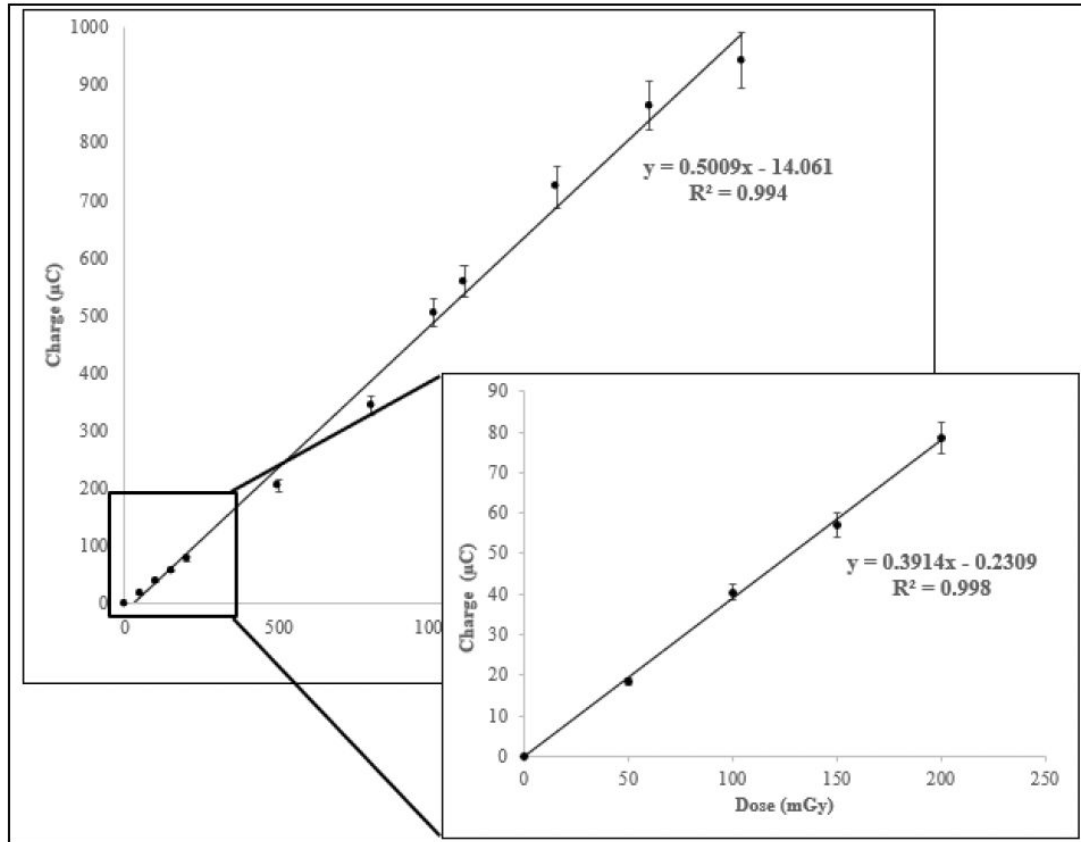


Figure 7: Dose linearity curve of TLD-100H using 6 MV energy in the dose ranges between 0 mGy and 2000 mGy with $\pm 5\%$ of error bar.

- TLD-100H showed nearly perfect linear response at low dose region from 0 mGy – 200 mGy with R^2 value of 0.998.
- TLD-100H was suitable to be used in low dose measurement.

Qualitative Analysis of Image Quality

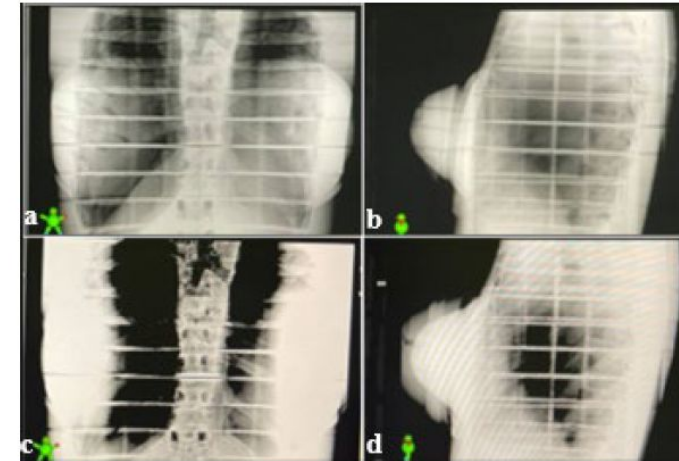


Figure 8: (a) AP and (b) Lat images of anthropomorphic phantom during MV EPID point dose measurement while (c) AP (d) Lat images of anthropomorphic phantom during kV orthogonal point dose measurement.

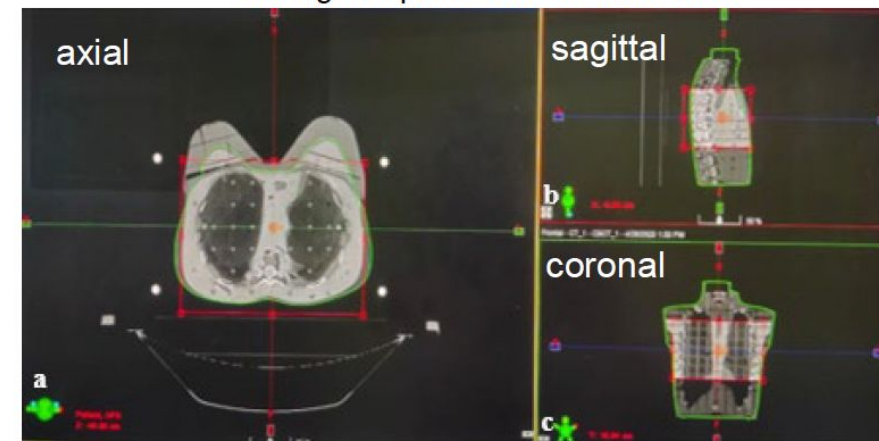


Figure 9: 3D images of anthropomorphic phantom at chest region acquired in kV CBCT point dose measurement.

Results & Discussion

Point Dose Analysis between 2D and 3D IGRT Techniques

Table 3: The percentage difference calculated between mean point doses at each point position in organs at chest region between 2D and 3D IGRT techniques. The p value was obtained from the one-way ANOVA.

Organs	Point label	Mean Dose (mGy)			Difference ^a (mGy)	Difference ^b (mGy)	p value
		MV EPID (mean ± SD)	kV orthogonal (mean ± SD)	kV CBCT (mean ± SD)			
Left lung	L1	40.674 ± 1.01	2.200 ± 0.21	11.686 ± 1.21	28.99	9.49	<0.001
	L2	44.451 ± 0.85	2.323 ± 0.24	10.489 ± 0.35	33.96	8.17	<0.001
Right lung	L3	33.586 ± 0.73	0.602 ± 0.04	10.862 ± 0.64	22.72	10.26	<0.001
	L4	26.324 ± 1.72	0.582 ± 0.06	11.072 ± 0.94	15.25	10.49	<0.001
Heart	H1	35.597 ± 0.01	0.996 ± 0.08	10.021 ± 0.15	25.58	9.03	<0.001
	H2	33.946 ± 1.32	0.832 ± 0.05	10.935 ± 0.73	23.01	10.10	<0.001
Left breast	B1	40.837 ± 0.04	0.669 ± 0.02	6.801 ± 0.38	34.04	6.13	<0.001
Right breast	B2	27.823 ± 0.33	0.222 ± 0.01	7.358 ± 0.49	20.47	7.14	<0.001
Skin	S1	23.811 ± 0.46	0.504 ± 0.05	10.218 ± 0.95	13.59	9.71	<0.001
	S2	22.414 ± 1.02	4.435 ± 0.16	6.590 ± 0.83	15.82	2.16	<0.001

*Difference^a refers to the difference calculated between the MV EPID and kV CBCT.

*Difference^b refers to the difference calculated between kV orthogonal and kV CBCT.

- There is significant difference of mean point dose between 2D and 3D IGRT techniques with p value < 0.001.

MV EPID vs kV CBCT

- MV EPID technique was reported contributing 20.47 - 34.04 mGy more mean point dose than kV CBCT technique, except for skin (13.59 mGy) and right lung (15.25 mGy).

- The possible reason is due to the different energy range and different image technique.^{2,3}

kV orthogonal vs kV CBCT

- kV CBCT contributed 6.13 - 10.49 mGy higher mean point dose to all the organs if compared to kV orthogonal technique, except skin with value of 2.16 mGy.⁴

- In 3D IGRT technique, the organs are exposed longer time due to acquisition of greater number of image projections for image reconstruction.⁵

Results & Discussion

Effective Dose Analysis between 2D and 3D IGRT Techniques

Table 4: The percentage difference of effective dose was calculated for MV EPID, kV orthogonal and kV CBCT.

Organs	Effective dose (mSv)			difference ^c (mSv)	difference ^d (mSv)	difference ^e (mSv)
	MV EPID	kV orthogonal	kV CBCT			
Left lung	5.108	0.271	1.331	4.84	3.78	1.06
Right lung	3.595	0.071	1.316	3.52	2.28	1.25
Heart	4.173	0.110	1.257	4.06	2.92	1.15
Left breast	4.900	0.080	0.816	4.82	4.08	0.74
Right breast	3.339	0.027	0.883	3.31	2.46	0.86
Skin	0.231	0.025	0.084	0.21	0.15	0.06

* Difference ^c represents the difference calculated between the MV EPID and kV orthogonal.

* Difference ^d represents the difference calculated between MV EPID and kV CBCT.

* Difference ^e represents the difference calculated between kV orthogonal and kV CBCT.

- MV EPID delivered effective dose in the ranges of 3.34 mSv to 5.11 mSv except for skin (0.23 mSv).

- kV orthogonal delivered effective dose less than 0.27 mSv in the organs at chest region.

- kV CBCT delivered effective dose in the ranges of 0.82 mSv to 1.33 mSv except for skin (0.084 mSv)

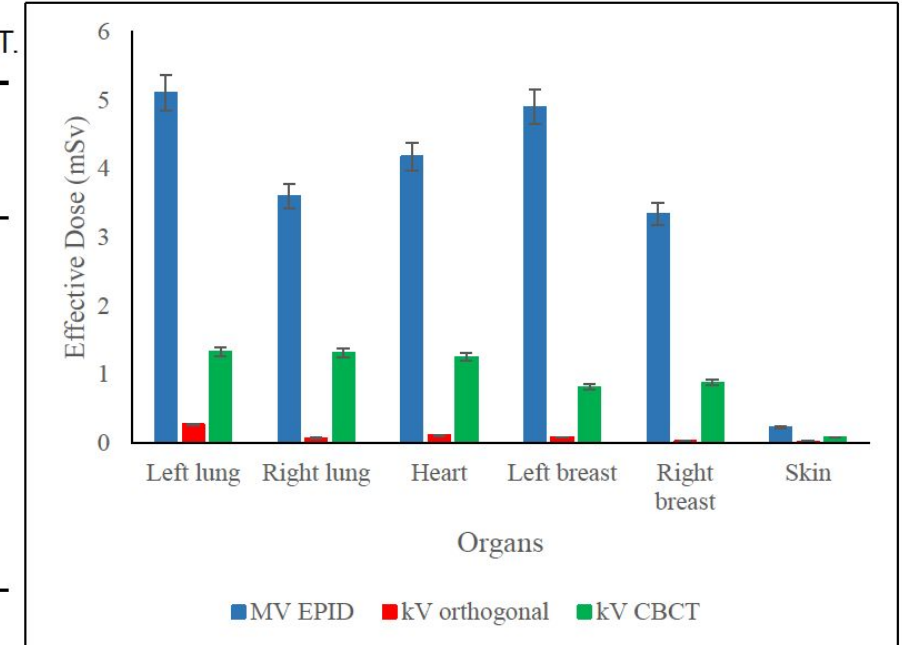


Figure 4: The bar graph of effective dose against all the organs at chest region among 2D and 3D IGRT techniques with $\pm 5\%$ error bar.

- The percentage error bars showed that no overlap between MV EPID, kV orthogonal and kV CBCT techniques.

- The overall effective dose at chest region reported by Alvarado et al. for kV CBCT (6.00mSv) and kV orthogonal technique (1.14mSv) was slightly higher than the overall effective dose for kV CBCT (5.69 mSv) and kV orthogonal (0.58 mSv).⁶

Imaging Dose Accumulation

Table 3: Accumulated point dose in organs at chest region for MV EPID, kV orthogonal and kV CBCT techniques in 8 fractions and 3 fractions of IGRT for VMAT and SBRT treatment technique, respectively.

Organ	Point Dose (mGy)					
	8 fractions (VMAT)			3 fractions (SBRT)		
	MV EPID	kV orthogonal	kV CBCT	MV EPID	kV orthogonal	kV CBCT
Right lung	268.688	4.816	86.896	100.758	1.806	32.586
Heart	284.776	7.968	80.168	106.791	2.988	30.063
Left breast	326.696	5.352	54.408	122.511	2.007	20.403
Right breast	222.584	1.776	58.864	83.469	0.666	22.074
Skin	179.312	35.480	52.720	67.242	13.305	19.770

- For VMAT and SBRT treatment techniques, the IGRT technique practiced in HUSM is kV CBCT.

VMAT

- The accumulated dose at OAR was ranged from 52.72 mGy – 86.90 mGy

SBRT

- The accumulated dose at OAR was ranged from 20.40 mGy to 32.59 mGy except for skin (19.77 mGy)

- The imaging dose accumulated from multiple fractions IGRT not necessary to be considered in treatment planning as it less than 5 % of therapeutic dose (60 Gy) prescribed for VMAT and SBRT treatment technique as mentioned in AAPM TG 180.

- In certain centres, the IGRT procedure with combined MV and kV energy ranges are used, for example MV EPID + kV CBCT technique, therefore the accumulated dose was total up from individual IGRT technique. ⁶

Image Quality

- kV energy generate better soft tissue contrast than MV energy but in certain case, MV EPID technique is sufficient to be used based on the bony landmark visualization.
- 3D IGRT produced volumetric OAR visualisation if compared to 2D IGRT.

Point Dose and Effective Dose between 2D and 3D IGRT Techniques

- There is a significant difference in mean point dose between 2D and 3D IGRT techniques with p-value < 0.001.
- kV CBCT contributed 6.13-10.49 mGy higher mean dose than kV orthogonal technique, in the contrary, MV EPID contributed 34.04 mGy higher mean point dose than kV CBCT
- The point dose and effective dose measured in the organs at chest region was increased in the order from kV orthogonal, kV CBCT and MV orthogonal technique.

Limitations

Limited number of TLD-100H

Point dose measurement does not represent the dose received by entire volume of the organ.

Result from reference-sized anthropomorphic phantom might overestimate/ underestimate the patients of different sizes, genders and ages

Future Recommendations

Measure the organ dose instead of point dose in the organ

Monte Carlo simulation study

References



1. Sung H, Ferlay J, Siegel RL, Laversanne M, Soerjomataram I, Jemal A, et al. Global Cancer Statistics 2020: GLOBOCAN Estimates of Incidence and Mortality Worldwide for 36 Cancers in 185 Countries. *Cancer J Clin*. 2021;71(3):209–49.
2. Sonke JJ, Aznar M, Rasch C. Adaptive Radiotherapy for Anatomical Changes. *Radiat Oncol* [Internet]. 2019;29(3):245–57. Available from: <https://doi.org/10.1016/j.semradonc.2019.02.007>
3. Ministry of Health M. Quality Assurance Program Manual in Radiotherapy Services. 2016. p. 7.
4. Murphy MJ, Balter J, Balter S, Bencomo JA, Das IJ, Jiang SB, et al. The management of imaging dose during image-guided radiotherapy: Report of the AAPM Task Group 75. *Med Phys*. 2007;34(10):4041–63.
5. Chew WZ, Jong WL, Jamaluddin Z, Fasha H, Kadri A, Mohamad A, et al. A single institutional audit of setup errors for 3DCRT rectal cancers. *J Heal Transl Med*. 2020;23(1):6–10.
6. Martin CJ, Kron T, Vassileva J, Wood TJ, Joyce C, Ung NM, et al. An international survey of imaging practices in radiotherapy. *Phys Medica* [Internet]. 2021;90:53–65. Available from: <https://doi.org/10.1016/j.ejmp.2021.09.004>
7. Park J, Yea JW, Park JW, Oh SA. Evaluation of the setup discrepancy between 6D ExacTrac and cone beam computed tomography in spine stereotactic body radiation therapy. *PLoS One* [Internet]. 2021;16(5 May):1–10. Available from: <http://dx.doi.org/10.1371/journal.pone.0252234>
8. Li GG, Mageras G, Dong L, Mohan R. Image-Guided Radiation Therapy. In: *Treatment Planning in Radiation Oncology*. Third edit. Lippincott Williams & Wilkins; 2015. p. 230–1.
9. Dzierma Y, Mikulla K, Richter P, Bell K, Melchior P, Nuesken F, et al. Imaging dose and secondary cancer risk in image-guided radiotherapy of pediatric patients. *Radiat Oncol*. 2018;13(1):1–14.
10. Stelczer G, Tatai-Szabó D, Major T, Mészáros N, Polgár C, Pálvölgyi J, et al. Measurement of dose exposure of image guidance in external beam accelerated partial breast irradiation: Evaluation of different techniques and linear accelerators. *Phys Medica*. 2019;63(December 2018):70–8.
11. Ding GX, Munro P. Radiation exposure to patients from image guidance procedures and techniques to reduce the imaging dose. *Radiat Oncol*. 2013;108(1):91–8.
12. Alvarado R, Booth JT, Bromley RM, Gustafsson HB. An investigation of image guidance dose for breast radiotherapy. *J Appl Clin Med Phys*. 2013;14(3):25–38.
13. Baptista M, Di Maria S, Vieira S, Pereira J, Pereira M, Vaz P. Organ dose measurements using an adult anthropomorphic phantom and risk estimation of cancer incidence from CBCT exposures. *Radiat Phys Chem*. 2020;171(November 2019).
14. Gibbons JP. Khan's *The Physics of Radiation Therapy*. Sixth edit. Wolters Kluwer Health; 2020. 968–974 p.
15. Ding GX, Alaei P, Curran B, Flynn R, Gossman M, Mackie TR, et al. Image guidance doses delivered during radiotherapy: Quantification, management, and reduction: Report of the AAPM Therapy Physics Committee Task Group 180. *Med Phys*. 2018;45(5):e84–99.
16. Podgorsak EB. Chapter 6: External Photon Beam: Physical Aspects. In: *Radiation oncology physics: A handbook for teachers and students*. 2005. p. 161–217.
17. Hill R, Healy B, Holloway L, Kuncic Z, Thwaites D, Baldock C. Advances in kilovoltage x-ray beam dosimetry. *Phys Med Biol*. 2014;59(6).
18. Li Y, Netherton T, Nitsch PL, Balter PA, Gao S, Klopp AH, et al. Normal tissue doses from MV image-guided radiation therapy (IGRT) using orthogonal MV and MV-CBCT. *J Appl Clin Med Phys*. 2017;19(3):52–7.
19. Duan YH, Gu H Le, Yang XH, Chen H, Wang H, Shao Y, et al. Evaluation of IGRT-Induced Imaging Doses and Secondary Cancer Risk for SBRT Early Lung Cancer Patients In Silico Study. *Technol Cancer Res Treat*. 2021;20:1–9.
20. Scarfe WC, Azevedo B, Toghyani S, Farman AG. Cone Beam Computed Tomographic imaging in orthodontics. *Aust Dent J*. 2017;62(1 Suppl):33–50.



THANK YOU
!